

Soil nitrous oxide emissions across the northern high latitudes

Naiqing Pan¹, Hanqin Tian^{1,2*}, Hao Shi³, Shufen Pan^{4,1}, Josep G. Canadell⁵, Jinfeng Chang⁶,
Philippe Ciais⁷, Eric A. Davidson⁸, Gustaf Hugelius^{9,10}, Akihiko Ito¹¹, Robert B. Jackson¹²,
Fortunat Joos¹³, Sebastian Lienert¹³, Dylan B. Millet¹⁴, Stefan Olin¹⁵, Prabir K. Patra¹⁶, Rona L.
Thompson¹⁷, Nicolas Vuichard⁷, Kelley C. Wells¹⁴, Chris Wilson^{18,19}, Yongfa You¹, Sönke
Zaehle²⁰

¹Center for Earth System Science and Global Sustainability, Schiller Institute for Integrated
Science and Society, Boston College, Chestnut Hill, MA, USA

²Department of Earth and Environmental Sciences, Boston College, Chestnut Hill, MA, USA

³State Key Laboratory of Urban and Regional Ecology, Research Center for Eco-Environmental
Sciences, Chinese Academy of Sciences, Beijing, China

⁴Department of Engineering and Environmental Studies Program, Boston College, Chestnut Hill,
MA, USA

⁵Global Carbon Project, CSIRO Oceans and Atmosphere, Canberra, Australian Capital Territory,
Australia

⁶ College of Environmental and Resource Sciences, Zhejiang University, Hangzhou, China

⁷Laboratoire des Sciences du Climat et de l'Environnement, LSCE, CEA CNRS, UVSQ
UPSACLAY, Gif sur Yvette, France

⁸Appalachian Laboratory, University of Maryland Center for Environmental Science, Frostburg,
MD, USA

⁹Department of Physical Geography, Stockholm University, Stockholm, Sweden

¹⁰ Bolin Centre for Climate Research, Stockholm University, Stockholm, Sweden

¹¹ National Institute for Environmental Studies, Tsukuba, Japan

¹² Department of Earth System Science, Woods Institute for the Environment, Precourt Institute
for Energy, Stanford University, Stanford, CA, USA

¹³ Climate and Environmental Physics, Physics Institute and Oeschger Centre for Climate Change Research, University of Bern, Bern, Switzerland

¹⁴ Department of Soil, Water, and Climate, University of Minnesota, St Paul, MN, USA

¹⁵ Department of Physical Geography and Ecosystem Science, Lund University, Lund, Sweden

¹⁶ Research Institute for Global Change, JAMSTEC, Yokohama, Japan

¹⁷ Norsk Institutt for Luftforskning, NILU, Kjeller, Norway

¹⁸ National Centre for Earth Observation, University of Leeds, Leeds, UK

¹⁹ Institute for Climate and Atmospheric Science, School of Earth & Environment, University of Leeds, Leeds, UK

²⁰ Max Planck Institute for Biogeochemistry, Jena, Germany

*Corresponding author: Hanqin Tian (hanqin.tian@bc.edu)

Geophysical Research Letters (Submitted on January 18, 2024)

Abstract

Nitrous oxide (N₂O) is the most important stratospheric ozone-depleting agent based on current emissions and the third largest contributor to increased net radiative forcing. Increases in atmospheric N₂O have been attributed primarily to enhanced soil N₂O emissions. Critically, contributions from soils in the Northern High Latitudes (NHL, >50°N) remain poorly quantified despite their vulnerability to permafrost thawing induced by climate change. An ensemble of six terrestrial biosphere models suggests NHL soil N₂O emissions doubled since the preindustrial 1860s, increasing on average by $2.0 \pm 1.0 \text{ Gg N yr}^{-1}$ ($p < 0.01$). This trend reversed after the 1980s because of reduced nitrogen fertilizer application in non-permafrost regions and increased plant growth due to CO₂ fertilization suppressed emissions. However, permafrost soil N₂O emissions continued increasing attributable to climate warming; the interaction of climate warming and increasing CO₂ concentrations on nitrogen and carbon cycling will determine future trends in NHL soil N₂O emissions.

Key Points

1. N₂O emissions from northern high latitudes during 1997-2014 are estimated at 0.5–1.3 Tg N yr⁻¹, and soil was the largest source.
2. Northern high latitudes soil N₂O emissions increased from $0.3 \pm 0.1 \text{ Tg N yr}^{-1}$ in 1861 to $0.6 \pm 0.3 \text{ Gg N yr}^{-1}$ in 2016.
3. Climate change stimulated soil N₂O emissions, while the increased atmospheric CO₂ concentration suppressed emissions.

Plain Language Summary

Soils in the Northern High Latitudes (NHL) store large amounts of nitrogen, providing rich substrates for the emissions of nitrous oxide (N_2O) which is a potent greenhouse gas and ozone-depleting substance. The NHL has experienced rapid climate warming in recent decades, however, to what extent climate and other environmental factors have affected soil N cycling and N_2O emissions in the NHL remain poorly quantified. This study has provided the first quantification of the magnitudes and spatiotemporal variations of soil N_2O emissions across the NHL and showed that the NHL contributed about 8% of the increase in global soil N_2O emissions since pre-industrial period (the 1860s). Our results further reveal that changes in climate and atmospheric CO_2 concentration not only largely affected historical variations in soil N_2O emissions from the NHL but also will determine their future trends. Our study suggests the need to better understand climate and CO_2 controls on soil N_2O emissions and nitrogen cycling across the NHL and to improve their representation in earth system models.

1 Introduction

Nitrous oxide (N_2O) emissions have received increasing attention, because N_2O is the most important stratospheric ozone-depleting agent based on current emissions [Ravishankara *et al.*, 2009] and the third largest contributor to net radiative forcing by greenhouse gases [Canadell *et al.*, 2021; Etminan *et al.*, 2016]. The large amount of nitrogen additions to soils since the preindustrial period has significantly increased the atmospheric N_2O burden [Canadell *et al.*, 2021; Tian *et al.*, 2020]. Denitrification and nitrification are two primary soil processes controlling N_2O production, which are regulated by multiple factors such as temperature, water availability, acidity, substrate availability and microbial diversity [Butterbach-Bahl *et al.*, 2013; Rees *et al.*, 2013].

91 Over the past 40 years, the northern high latitudes, usually defined as the region north of 50°N
92 [Watts *et al.*, 2012], have experienced climate warming at a rate faster than anywhere else on Earth
93 [Rantanen *et al.*, 2022], a trend expected to continue in the coming decades [Masson-Delmotte *et*
94 *al.*, 2021]. Therefore, there is an urgent need to understand and quantify how changes in climate
95 and other environmental factors since the pre-industrial era have affected soil N₂O emissions from
96 the NHL and thus have shaped the strength of climate-biogeochemical feedback.

97 The terrestrial nitrogen cycle in the NHL is closely related with permafrost, which underlays more
98 than 60% of the area [Brown *et al.*, 1997]. Although large N stocks are stored in this region [Harden
99 *et al.*, 2012; Hugelius *et al.*, 2020], the associated soil N₂O emissions have received little attention
100 because they were considered to be small due to limited microbial activity and low mineralization
101 rates under low-temperature and waterlogged conditions [Voigt *et al.*, 2020]. However, recent in-
102 situ studies found that both barren and vegetated soils in the NHL can emit substantial amounts of
103 N₂O [Marushchak *et al.*, 2011; Marushchak *et al.*, 2021; Repo *et al.*, 2009; Voigt *et al.*, 2017b].
104 Meanwhile, Arctic amplification, the phenomenon that climate change is amplified in the NHL, is
105 projected to continue in the 21st century [Christensen *et al.*, 2013; Pithan and Mauritsen, 2014]
106 with further implications for N₂O emissions: first, a large amount of immobile N stored in
107 permafrost becomes available for decomposition and remobilization after permafrost thawing;
108 second, rapid warming enhances N mineralization and promotes nitrification and denitrification;
109 and third, warming may also promote biological nitrogen fixation (BNF), increasing ecosystem N
110 availability and thereby potentially also N₂O production. Field experiments also confirm that
111 warming can significantly increase N₂O emissions from permafrost-affected soils [Cui *et al.*, 2018;
112 Voigt *et al.*, 2017b; Wang *et al.*, 2017].

Another influential factor for N₂O emissions in the NHL is the atmospheric CO₂ concentrations. Elevated atmospheric CO₂ concentrations do not have significant direct effects on reactive N flows controlling N₂O production, but can indirectly affect soil N₂O emissions by changing plant nitrogen uptake and root exudates due to enhanced plant growth [Usyskin-Tonne *et al.*, 2020]. On one hand, elevated atmospheric CO₂ promotes plant growth and thus more absorption of soil mineral N, restricting N₂O production [Tian *et al.*, 2019]. On the other hand, it may stimulate denitrification-derived N₂O emissions by increasing plant biomass and hence carbon substrate availability [Kammann *et al.*, 2008]. Additionally, elevated CO₂ can affect soil moisture by improving plant water-use efficiency, which can increase anaerobic conditions that stimulate denitrification [Butterbach-Bahl *et al.*, 2013]. Such contrasting effects of elevated CO₂ concentrations on N₂O emissions have been observed in field experiments [Dijkstra *et al.*, 2012; Liu *et al.*, 2018; X Sun *et al.*, 2018] but the magnitude of the CO₂ effect on northern soil N₂O emissions remains poorly understood.

Here, we investigated NHL soil N₂O emissions using six process-based terrestrial biosphere models (TBMs) from the global N₂O Model Intercomparison Project (NMIP) [Tian *et al.*, 2018]. Using factorial simulation experiments, we quantified the contributions of different driving factors, particularly climate change and rising atmospheric CO₂, to the variations in soil N₂O emissions during 1861-2016. Statistical methods were further employed to disentangle the effects of temperature and precipitation on soil N₂O emissions. We also compared bottom-up (BU, including process-based TBMs for soil emissions and emission factor approaches for non-soil emissions) estimates of N₂O emissions with those of three atmospheric inversion frameworks (top-down, TD) [Rona L. Thompson *et al.*, 2019] to investigate the uncertainties in current estimates of N₂O emissions from the NHL.

2 Materials and methods

2.1 Data sources

2.1.1 Soil N₂O emissions

An ensemble estimate of soil N₂O emissions from the NHL was derived from simulations by the six TBMs that participated in the NMIP: (1) DLEM [Tian *et al.*, 2015], (2) LPJ-GUESS [Olin *et al.*, 2015], (3) LPX-Bern [Joos *et al.*, 2020], (4) O-CN [Zaehle *et al.*, 2011], (5) ORCHIDEE-CNP [Goll *et al.*, 2017; Y Sun *et al.*, 2021], and (6) VISIT [Inatomi *et al.*, 2010]. Each model performed a subset of seven simulations (S0-S6) to quantify N₂O emissions from both agricultural and natural soils, and to disentangle the effects of multiple environmental factors on N₂O emissions (Table S1). The differences between pairs of simulations, i.e. S1-S2, S2-S3, S3-S4, S4-S5, S5-S6, and S6-S0, were used to evaluate the effects of manure N, mineral N fertilizer, atmospheric N deposition, land use and land cover change (LULCC), atmospheric CO₂ concentration, and climate, respectively. More information about the model simulation protocol and forcing data can refer to Tian *et al.* [2018]. Among the six NMIP models, LPJ-GUESS and LPX-Bern have dedicated permafrost modules and consider freeze-thaw processes; O-CN lacks an explicit permafrost representation but describes freeze-thaw cycles; the other models have no explicit representation of the permafrost layer or freeze-thaw processes.

2.1.2 Fire-induced N₂O emissions and non-soil anthropogenic N₂O emissions

N₂O emissions from biomass burning were from the GFED4.1s dataset. N₂O emissions from non-soil anthropogenic sources were obtained from EDGAR 6.0 [Crippa *et al.*, 2019]. EDGAR non-soil anthropogenic emissions were combined with GFED biomass burning emissions and with

NMIP soil emissions to constitute BU estimates of total N₂O emissions, aiming to make comparison with TD estimates.

2.1.3 Top-down N₂O emission estimates

Three independent atmospheric inversion models were used: GEOS-Chem [Wells *et al.*, 2018], INVICAT [Wilson *et al.*, 2014] and MIROC4-ACTM [Patra *et al.*, 2018; Patra *et al.*, 2022]. GEOS-Chem and INVICAT used the same prior estimates: soil emissions from the O-CN model, biomass burning emissions from GFEDv4.1s, and non-soil anthropogenic emissions from EDGAR v4.2FT2010. The MIROC4-ACTM prior used natural soil emissions from the VISIT model, and all anthropogenic emissions from EDGAR 4.2. The MIROC4-ACTM prior included agricultural burning but did not explicitly include wildfire emissions. All models used the Bayesian inversion framework to find the optimal emissions that provide the best agreement to observed N₂O mixing ratios while being coupled to an atmospheric transport model.

2.2 Statistical methods

The path analysis model (PAM) was used to investigate how climatic factors affected permafrost soil N₂O emissions. PAM can deal with complex relationships among multiple independent and dependent variables, and disentangle direct and indirect effects of the explanatory variables on the response variable [Alwin and Hauser, 1975; You and Pan, 2020]. Here, we developed the conceptual model by specifying the relationships between climatic factors and soil N₂O emissions and considering the interactions between these factors. We also conducted partial correlation analysis between soil N₂O emissions and temperature/precipitation. The temporal sensitivities of

soil N₂O emissions to temperature and precipitation were fitted using a multiple regression model. The Mann–Kendall test was used to assess the significance of trends in N₂O emissions.

3 Results

3.1 Spatiotemporal variations of soil N₂O emissions since the 1860s

Multi-model ensemble estimates show that soil N₂O emissions from the NHL increased from 312±125 Gg N yr⁻¹ in 1861 to 605±269 Gg N yr⁻¹ in 2016 (Fig.1a), with an average increase rate of 2.0±1.0 Gg N yr⁻¹ ($p<0.01$). Soil N₂O emissions from non-permafrost regions dominated the temporal variations of total NHL emissions, which were relatively stable over the first five decades, then rapidly increased from the 1920s to the 1980s, and peaked in the 1980s. In the late 1980s and early 1990s, northern soil N₂O emissions drastically decreased and fluctuated afterwards. Meanwhile, soil N₂O emissions from permafrost regions showed different temporal dynamics; they remained relatively stable before the 1980s, and rapidly increased thereafter. In the 1860s, the highest emission density occurred in Central Europe. During 1861-2016, soil N₂O emissions from most regions significantly increased. In the recent decade (2007-2016), Western Europe had the highest emission density (Fig.1b-d), and more than half of the soil N₂O emissions were from croplands (Fig. S2). During 1861-1980, the fastest increase in N₂O emissions occurred in Western and Central Europe where the average increase exceeded 2×10^{-4} g N m⁻² yr⁻¹ (Fig.1e). However, trends in soil N₂O emissions have largely changed since 1980, with emissions significantly decreasing in Eastern Europe and Russia but rapidly increasing in Siberia and Southern Canada (Fig.1f).

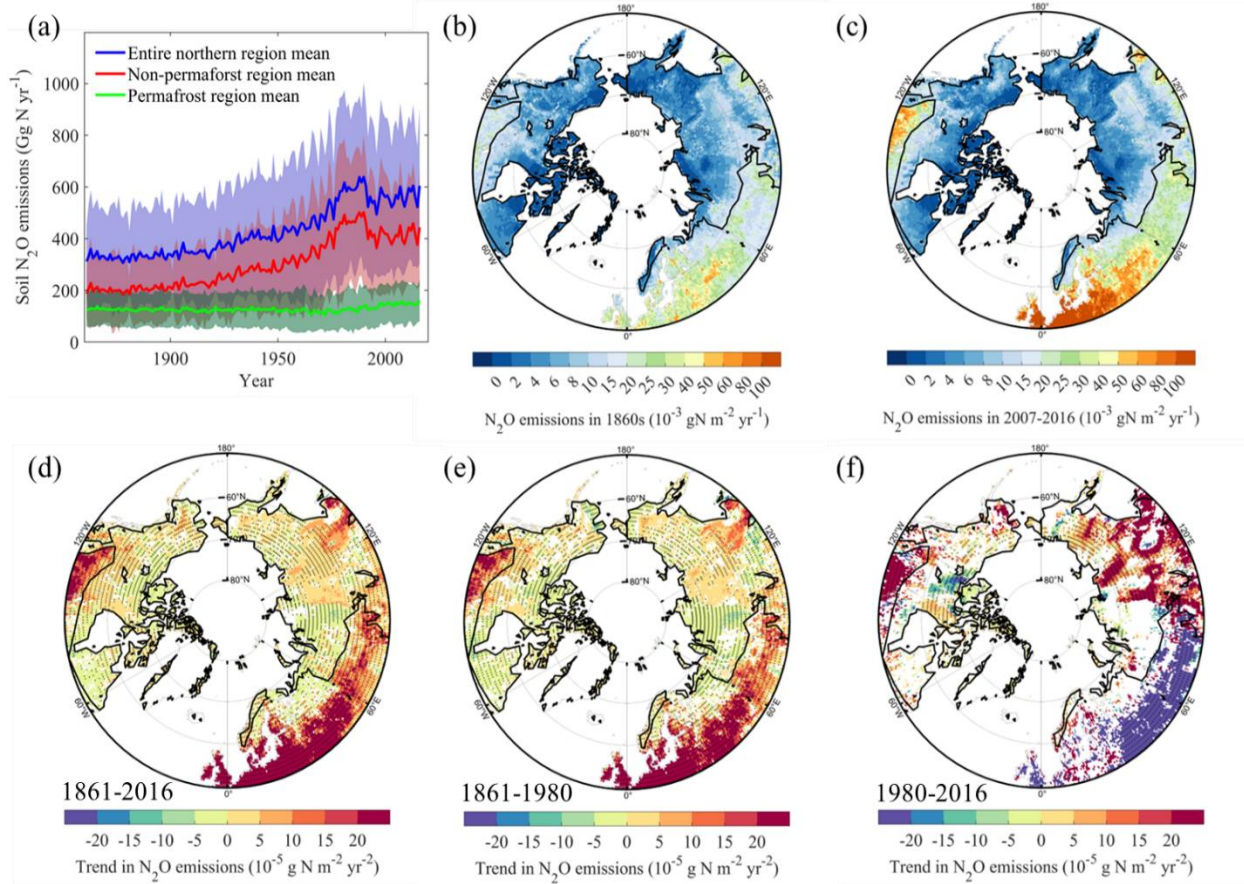


Fig. 1: (a) Changes in soil N₂O emissions from the NHL, the shaded area indicates one standard deviation of all estimates. (b) and (c) show spatial pattern of mean annual soil N₂O emissions during the 1860s and 2007-2016, respectively. Trends in soil N₂O emissions during 1861-2016 (d), 1861-1980 (e), and 1980-2016 (f); grids with non-significant trends ($p \geq 0.05$) were excluded, and stippling indicates where a majority of models (at least 4 out of 6) agree on the sign of the trend.

3.2 Contributions of different driving factors to soil N₂O emissions during 1861-2016

Our results derived from factorial simulations suggested that increasing atmospheric CO₂ concentrations reduced NHL soil N₂O emissions, while the other five factors stimulated N₂O emissions (Fig. 2a). Climate change played a dominant role in stimulating N₂O emissions before

the 1930s and N inputs made increasing contributions from the 1940s to the 1980s. From the 1860s to the 1980s, fertilizer application contributed 53% to the increase in emissions, followed by atmospheric N deposition (26%), manure N application (15%), climate change (12%), and land use change (5%). The effect of increased atmospheric CO₂ (-10%) almost offset that of climate change. Since the 1980s, the role of anthropogenic N inputs in stimulating N₂O emissions weakened gradually; by contrast, drastic warming and wetting made climate change increasingly important (Fig. S3). Over the entire study period, climate change made the second largest contribution (37%) to the increase of NHL soil emissions after N fertilizer application (42%). Climate change had a larger relative contribution to the emission increase in permafrost regions (Fig. 2c) than in non-permafrost regions. During 1861-2016, climate change contributed 114% (partly offset by the negative CO₂ effect) to the emission increase in permafrost regions, which was stronger than in non-permafrost regions (28%) (Fig. 2d). All individual models agreed that climate change made a larger relative contribution to emission increases in permafrost regions than in non-permafrost regions, and that the effects of climate change have increased since the 1980s (Fig. S4-6). In most northern regions, trends in soil N₂O emissions were dominated by climate change; fertilizer only dominated trends in Western Europe and some intensive agricultural lands over Eastern Europe, Russia, and south Canada, while atmospheric N deposition dominated trends in part of Central and Eastern Europe. Regions dominated by other factors were relatively small (Fig. 2b).

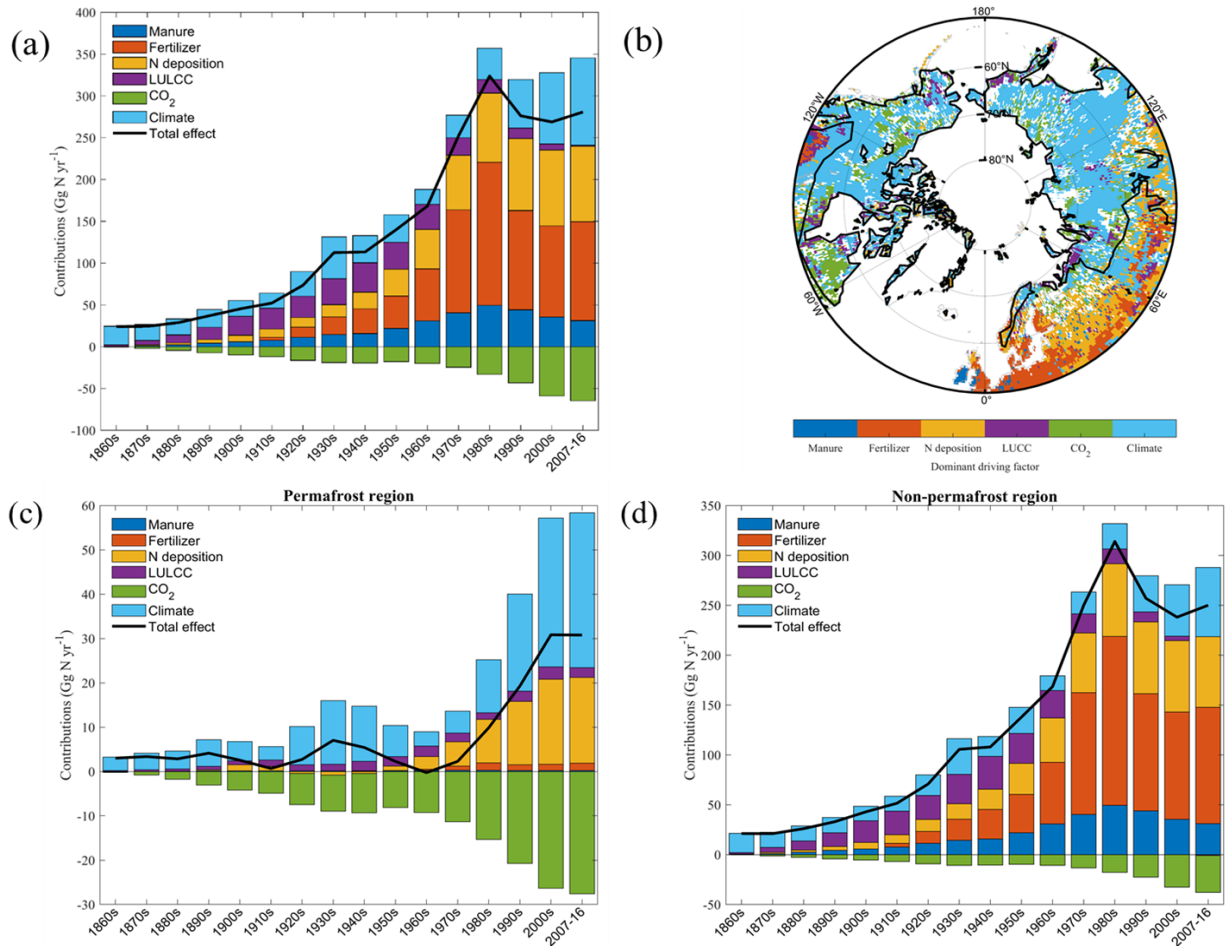


Fig. 2: (a) Decadal variations in the contributions of different driving factors. (b) Distribution of dominant driving factors of soil N₂O emissions during 1861-2016; grids with non-significant trends were excluded. Contributions of different driving factors to soil N₂O emissions from permafrost regions (c) and non-permafrost regions (d).

3.3 Effects of temperature and precipitation on soil N₂O emissions

Temperature and precipitation changes alter soil microclimate, nutrient availability and microbial ecology, thereby influencing N₂O emissions [Dalal and Allen, 2008]. For the entire NHL, both temperature and precipitation significantly increased during 1901-2016, with rates of 0.14 °C per decade and 0.38 mm yr⁻¹ (10% total increase since the 1900s), respectively (Fig. S3). According

to multiple regression model results, the sensitivities of soil N₂O emissions to temperature and precipitation were 29 ± 21 Gg N °C⁻¹ and 0.4 ± 0.7 Gg N mm⁻¹ during 1901-2016, suggesting that warming and wetting increased soil N₂O emissions by 48 ± 35 Gg N yr⁻¹ and 15 ± 26 Gg N yr⁻¹, respectively. The path analysis model also suggested that warming contributed more to soil N₂O emission increases than wetting (Fig. S7). Both warming and wetting have accelerated since 1980 (Fig. S3, S8, S9), with average rates of 0.38 °C per decade and 0.57 mm yr⁻², respectively. At the same time, the sensitivities of soil N₂O emissions to temperature and precipitation increased to 38 ± 22 Gg N °C⁻¹ and 1.2 ± 0.8 Gg N mm⁻¹, respectively. These two factors together led to the large climate effects in the recent four decades.

Soil N₂O emissions were positively correlated with temperature in most northern regions (Fig. S10a). Compared with the 1901-1980 period, warming after 1980 was more pronounced and prevalent (Fig. S8-9), which enhanced biological N fixation and net N mineralization and further promoted nitrification and denitrification (Fig. S11). During the study period, most of the NHL experienced significant warming (Fig. S10c), indicating that warming universally stimulated N₂O emissions in this region. Recent manipulation experiments also suggest that warming can significantly increase soil N₂O emissions from the NHL [Cui *et al.*, 2018; Voigt *et al.*, 2017b; Wang *et al.*, 2017]. Unlike temperature, the correlation between soil N₂O emissions and precipitation varied spatially (Fig. S10b). Although a large area of the NHL experienced significant wetting (Fig. S10d), the positive effects of wetting on emissions from Eastern Europe, central Canada and Siberia were partly counteracted by the negative effects in Northern Europe and northwestern Russia, which explained why precipitation had a smaller effect than temperature on the regional total emissions.

3.4 Declining soil N₂O emissions since the 1980s

Soil N₂O emissions from the NHL rapidly increased before the 1980s, however, declined thereafter. Although total BNF over the NHL increased since 1980 (Fig. S12), the ensemble mean of soil N₂O emissions from the NHL decreased at an average rate of -1.1 GgN yr⁻¹ ($p < 0.05$) during 1980-2016 (Fig. 3a). The rapid decline in emissions during 1988-1996 was due to reduced fertilizer application, after which period the negative effect of CO₂ fertilization was enhanced (Fig. S14). The most pronounced decline occurred in Eastern Europe and Russia (Fig. 1f), mainly caused by the sharp decrease in external nitrogen inputs due to the collapse of the Soviet Union (Fig. S14). Concurrently, soil emissions from Siberia and Southern Canada significantly increased, due to climate change and nitrogen enrichment, respectively (Fig. S14). Soil N₂O emissions fluctuated after 1998 because the positive climate effect was counteracted by combined effects of fertilizer application, CO₂ and land use change.

The dominant drivers of negative effects differed between permafrost and non-permafrost regions. In permafrost regions, elevated CO₂ concentration was the only factor suppressing soil N₂O emissions and counteracted more than half of the climate-induced emissions (Fig. 3b). By contrast, reduced N fertilizer application, elevated CO₂ concentration and land use change jointly reduced emissions from non-permafrost regions (Fig. 3c). For the entire NHL, the atmospheric CO₂-induced decline in soil N₂O emissions surpassed the effect of reduced fertilizer application over the recent decade. Elevated atmospheric CO₂ significantly suppressed N₂O emissions in most northern regions (Fig. S14). Since the 1980s, increased atmospheric CO₂ concentrations stimulated terrestrial gross primary production (Fig. S15a, c), thus enhancing plant nitrogen uptake (Fig. S15b, d) and reducing the availability of soil inorganic nitrogen, which finally suppressed N₂O emissions.

The largest stimulation effect of CO₂ on vegetation growth and nitrogen uptake occurred in the boreal forests, where the CO₂-induced suppression of N₂O emissions was the most pronounced. Enhanced vegetation growth in the NHL has been reported in previous studies [Berner *et al.*, 2020; Myers-Smith *et al.*, 2020; Virkkala *et al.*, 2021]. Reduced N₂O emissions due to enhanced plant growth and nitrogen uptake is also consistent with field observations in the NHL [Gong and Wu, 2021; Marushchak *et al.*, 2011; Stewart *et al.*, 2012].

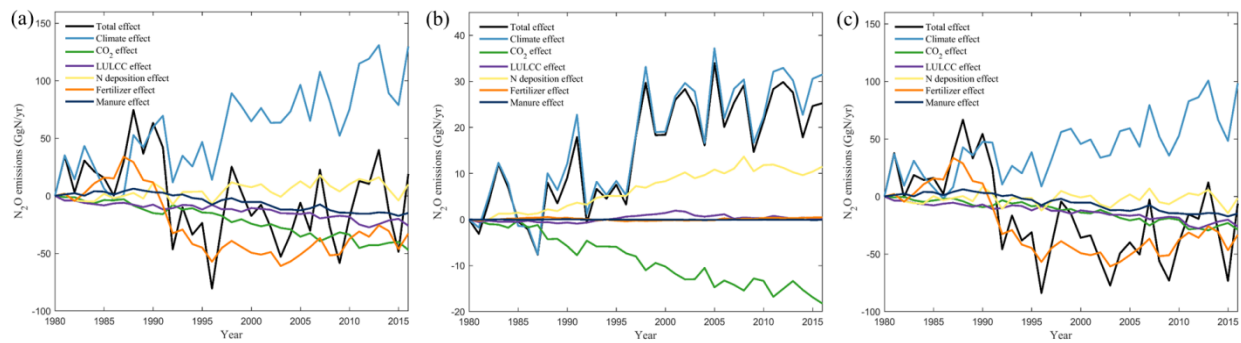


Fig. 3: Contributions of different driving factors in the entire NHL (a), permafrost regions (b), and non-permafrost regions (c) during 1980-2016.

3.5 Comparison with TD estimates

Using the current N₂O observation network, TD models estimate total N₂O emissions with its spatial distribution across the land but cannot well quantify the contributions of different sources. With the aim of comparing BU estimates with TD estimates, we added N₂O emissions from soil, biomass burning and non-soil anthropogenic sources (Fig. S16) together to constitute BU estimates of total N₂O emissions. According to the resulting BU estimates, soil was the largest source of N₂O emissions in the NHL (mean value: 572 Gg N yr⁻¹ during 1998-2014), followed by non-soil anthropogenic sources (280 Gg N yr⁻¹) and biomass burning (143 Gg N yr⁻¹). Both BU and TD

approaches indicated similar spatial emission patterns (Fig. 4), but the ensemble mean of total BU estimate (995 ± 267 Gg N yr⁻¹) was substantially higher than the TD estimate (668 ± 134 Gg N yr⁻¹) for the overlapping 1998-2014 period. Both TD and BU approaches revealed that the total N₂O emissions had no significant trend during this period ($p > 0.05$). Removing N₂O emitted by biomass burning and non-soil anthropogenic sources from the TD estimates, the remaining N₂O exhibited a decreasing trend during 1998-2014 (from -10.0 to -3.2 Gg N yr⁻², mean -7.3 Gg N yr⁻²), implying that the TD models also suggest a decreasing trend in NHL soil N₂O emissions.

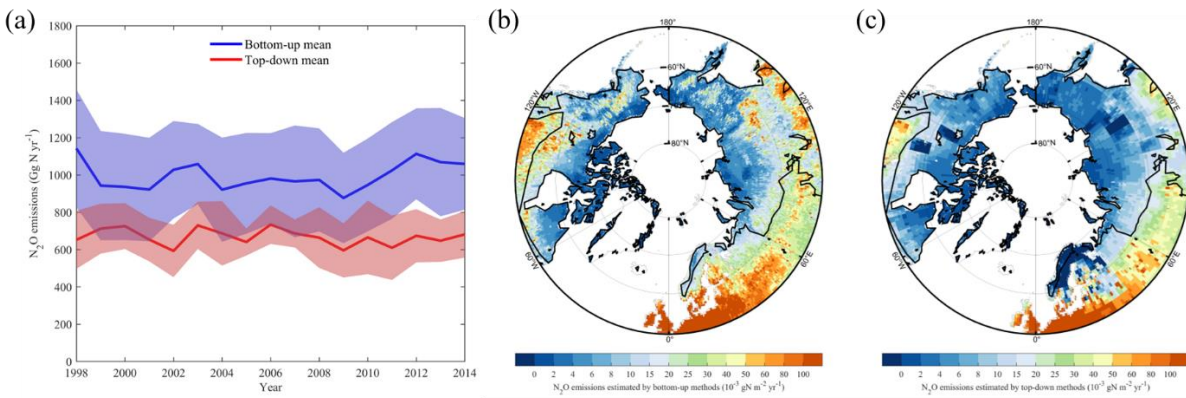


Fig. 4: (a) Comparison between TD and BU estimates of total N₂O emissions, the lines represent the ensemble means and the shaded areas indicate one standard deviation of model estimates. Spatial pattern of total N₂O emissions estimated by BU (b) and TD (c) approaches.

3.6 Comparison with empirical estimates

Based on site-level observation data, Voigt *et al.* [2020] estimated soil N₂O emissions from permafrost regions using a simple extrapolation method, and proposed that peatlands had the highest N₂O emissions among natural permafrost ecosystems. However, these extrapolation-based estimates have large uncertainties, with the implied annual soil N₂O emissions from the NHL ranging from 140 to 1030 Gg N⁻¹. In particular, estimates based on mean fluxes are an order of

magnitude larger than those based on median fluxes because of several N₂O emission hot spots. Combining observed peatland annual fluxes and peatland distribution maps, *Hugelius et al.* [2020] estimated a much smaller northern peatland source of 22 ± 5 Gg N·y⁻¹, with only half of that peatland area being permafrost. This suggests a smaller source than the estimates of *Voigt et al.* [2020]. NMIP estimates of soil N₂O emissions from the permafrost regions are close to the lower-limit of estimates by *Voigt et al.* [2020], and have smaller uncertainty range (0.11-0.26 Tg N⁻¹, mean 0.17 Tg N⁻¹), which partly reflect the usage of unified model input data. Soil N₂O emissions from non-permafrost regions are largely controlled by fertilizer and manure applications. According to NMIP models, the average emission factors of fertilizer and manure in non-permafrost regions during 1980-2016 were 1.4% and 1.7%, respectively. Both factors were positively correlated with temperature and precipitation, suggesting positive interactions between nitrogen additions and climate change [*Tian et al.*, 2020].

4 Discussion

Our study provides a first estimate of soil N₂O emissions from the NHL, although large uncertainties remain in both TD and BU approaches (Fig. S17, S18). Since the process-based models used in this study were driven by the same input data, differences were mainly induced by missing or uncertain representation of important processes such as seasonal freeze-thaw cycles and permafrost thaw [*Risk et al.*, 2013], BNF [*Meyerholt et al.*, 2020] and reactive N flows through ecosystems [*Butterbach-Bahl et al.*, 2013], and critical information such as timing and frequency of fertilizer application [*Nishina et al.*, 2017]. Several NMIP models do not include an explicit permafrost layer or freeze-thaw processes; inclusion of such factors would enable better representation of “hot spots” and “hot moments” soil N₂O emissions in the NHL [*Voigt et al.*, 2020;

Wagner-Riddle *et al.*, 2017]. Current process-based TBMs also have insufficient representation of the upland thermokarst formation [Yang *et al.*, 2018] and fine-grained landscape structure of arctic ecosystems (e.g., landscape elements that are ultra-emitters of N₂O such as non-vegetated organic soil). Integrating sub-grid scale information and processes into models may provide a solution for fine-grained physical-hydrological modelling. As revealed by Voigt *et al.* [2020], peatlands have the highest N₂O emission rate in permafrost regions. It is thus important for process-based TBMs to explicitly consider peatland thermal, hydrological, and biogeochemical processes.

TD estimates have a stronger dependence on the prior fluxes in NHL where atmospheric N₂O measurements are sparse [Nevison *et al.*, 2018; Rona Louise Thompson *et al.*, 2014; Rona L. Thompson *et al.*, 2019]. In this study, the average prior N₂O flux employed in the TD models (846±141 Gg N yr⁻¹) was lower than our BU estimates (955±267 Gg N yr⁻¹). These low prior N₂O fluxes, as well as lower TD emissions in summer compared to the BU estimates, are the likely causes of the lower TD estimates (Fig. S18). Differing prior N₂O fluxes between the inversions (see methods) also lead to somewhat varying inversion estimates. Using the ensemble mean NMIP soil emission estimates as prior for the TD inversions may improve model agreement. The total prior ocean flux also has important impacts on the magnitude of the terrestrial flux. However, there have been few observational constraints on the ocean source until recently [Patra *et al.*, 2022]. The sparseness of atmospheric observations over both land and ocean north of 50°N and systematic model errors in stratosphere-troposphere exchange increase the uncertainty in TD estimates. Building denser regional N₂O monitoring networks and launching (regular) aircraft campaigns in the NHL will help better constrain inversion models [Bisht *et al.*, 2021].

Our results suggest that the NHL contributed approximately 8% of the increase in global soil N₂O emissions during 1861-2016 [Tian *et al.*, 2019]. Warming and wetting stimulated NHL soil N₂O emissions, while elevated CO₂ concentrations suppressed emissions (through increased plant growth and larger uptake of soil N), findings that are in line with field observations [Cui *et al.*, 2018; Dijkstra *et al.*, 2012; Gong and Wu, 2021; Marushchak *et al.*, 2011; Voigt *et al.*, 2017a]. From 1980-2016 when warming was strongest, the NHL contributed 14% of global climate effect enhancing soil N₂O emissions. Under the SSP370 and SSP585 scenarios, CMIP6 climate models predict that the mean temperature of the NHL will increase by 6.2 (4.1-9.8) °C and 7.8 (5.5-12.1) °C, respectively, during 2015-2100; the mean precipitation will increase by 96 (65-177) mm yr⁻¹ and 129 (51-206) mm yr⁻¹, respectively (Fig. S19). If the sensitivities of soil N₂O emissions to temperature and precipitation in the future are consistent with historical values, future climate change alone will substantially increase NHL soil N₂O emissions. However, atmospheric CO₂ concentrations also rapidly increase under SSP370 and SSP585 scenarios (Fig. S20), potentially offsetting a significant fraction of the positive climate effect if arctic vegetation continues to take up more carbon and nitrogen with elevated CO₂. Uncertainties arise regarding the degree of recycling of that extra nitrogen uptake in soils by mineralization. The magnitude of the future CO₂ effect is also highly uncertain [Walker *et al.*, 2021], and how it will affect future northern N₂O emissions requires further study. Reconstructions from ice cores show that global N₂O emissions increased over the last deglaciation when the climate warmed, CO₂ increased, and land carbon inventories grew in size, providing evidence for a net positive relationship between past warming, CO₂, land carbon, stocks, and N₂O emissions at the global scale [Fischer *et al.*, 2019; Joos *et al.*, 2020].

Since the NMIP project did not design simulation experiments to separate the effects of temperature and precipitation on soil N₂O emissions, we used statistical methods to explore these relationships. However, the collinearity between temperature and precipitation variations may undermine the reliability of the inferred sensitivities of soil N₂O emissions to temperature and precipitation. Future model intercomparison projects need to design simulations to disentangle the effects of temperature and precipitation.

Acknowledgements

This study was resulted from NMIP (global N/N₂O Model Intercomparison Project) co-sponsored by Global Carbon Project and International Nitrogen Initiative. This work contributes to the REgional Carbon Cycle Assessment and Processes-2 of the Global Carbon Project. H.T., N. Pan, S. Pan acknowledge funding support from NSF (grant nos. 1903722, 1922687); PKP is partly funded by the Arctic Challenge for Sustainability phase II (ArCS-II; JPMXD1420318865) Projects of the Ministry of Education, Culture, Sports, Science and Technology (MEXT); KCW and DBM acknowledge support from NASA (Grant #NNX17AK18G) and NOAA (Grant #NA13OAR4310086).

Data availability statement

EDGAR 6.0 dataset is available at https://edgar.jrc.ec.europa.eu/dataset_ghg60. GFED4.1s dataset is available at <https://www.geo.vu.nl/~gwerf/GFED/GFED4/>. Soil N₂O emissions, terrestrial GPP and plant nitrogen uptake estimated by NMIP models and top-down N₂O emission are available at <https://datadryad.org/stash/share/isclqpURaZ5GJLLok3LCvjBrQ20ybXX7M3dQzuVWFCK>

Author contributions

H.T. initiated and designed this research, N.P. conducted data analysis and synthesis, N.P. and H.T. drafted the manuscript. All co-authors contributed to the writing and development of the manuscript.

Competing interests

The authors declare no competing interests.

References

- Alwin, D. F., and R. M. Hauser (1975), The decomposition of effects in path analysis, *American sociological review*, 37-47.
- Berner, L. T., R. Massey, P. Jantz, B. C. Forbes, M. Macias-Fauria, I. Myers-Smith, T. Kumpula, G. Gauthier, L. Andreu-Hayles, and B. V. Gaglioti (2020), Summer warming explains widespread but not uniform greening in the Arctic tundra biome, *Nature communications*, 11(1), 1-12.
- Bisht, J. S. H., T. Machida, N. Chandra, K. Tsuboi, P. K. Patra, T. Umezawa, Y. Niwa, Y. Sawa, S. Morimoto, and T. Nakazawa (2021), Seasonal Variations of SF₆, CO₂, CH₄, and N₂O in the UT/LS Region due to Emissions, Transport, and Chemistry, *Journal of Geophysical Research: Atmospheres*, 126(4), e2020JD033541.
- Brown, J., O. J. Ferrians Jr, J. A. Heginbottom, and E. S. Melnikov (1997), Circum-arctic map of permafrost and ground ice conditions.
- Butterbach-Bahl, K., L. Baggs, M. Dannenmann, R. Kiese, and S. Zechmeister-Boltenstern (2013), Nitrous oxide emissions from soils: How well do we understand the processes and their controls?, *Philosophical transactions of the Royal Society of London. Series B, Biological sciences*, 368, 20130122.
- Canadell, J. G., P. M. S. Monteiro, M. H. Costa, L. C. Da Cunha, P. M. Cox, V. Alexey, S. Henson, M. Ishii, S. Jaccard, and C. Koven (2021), Global carbon and other biogeochemical cycles and feedbacks, edited.
- Christensen, J. H., K. K. Kanikicharla, E. Aldrian, S. I. An, I. F. A. Cavalcanti, M. de Castro, W. Dong, P. Goswami, A. Hall, and J. K. Kanyanga (2013), Climate phenomena and their relevance for future regional climate change, in *Climate change 2013 the physical science basis: Working group I contribution to the fifth assessment report of the intergovernmental panel on climate change*, edited, pp. 1217-1308, Cambridge University Press.
- Crippa, M., G. Oreggioni, D. Guizzardi, M. Muntean, E. Schaaf, E. Lo Vullo, E. Solazzo, F. Monforti-Ferrario, J. G. J. Olivier, and E. Vignati (2019), Fossil CO₂ and GHG emissions of all world countries, *Publication Office of the European Union: Luxembourg*.
- Cui, Q., C. Song, X. Wang, F. Shi, X. Yu, and W. Tan (2018), Effects of warming on N₂O fluxes in a boreal peatland of Permafrost region, Northeast China, *Science of The Total Environment*, 616-617, 427-434.
- Dalal, R. C., and D. E. Allen (2008), Greenhouse gas fluxes from natural ecosystems, *Australian Journal of Botany*, 56(5), 369-407.
- Dijkstra, F. A., S. A. Prior, G. B. Runion, H. A. Torbert, H. Tian, C. Lu, and R. T. Venterea (2012), Effects of elevated carbon dioxide and increased temperature on methane and nitrous oxide fluxes: evidence from field experiments, *Frontiers in Ecology and the Environment*, 10(10), 520-527.

438 Etminan, M., G. Myhre, E. J. Highwood, and K. P. Shine (2016), Radiative forcing of carbon dioxide,
 439 methane, and nitrous oxide: A significant revision of the methane radiative forcing, *Geophysical Research*
 440 *Letters*, 43(24), 12-614.
 441 Fischer, H., et al. (2019), N₂O changes from the Last Glacial Maximum to the preindustrial – Part 1:
 442 Quantitative reconstruction of terrestrial and marine emissions using N₂O stable isotopes in ice cores,
 443 *Biogeosciences*, 16(20), 3997-4021.
 444 Goll, D. S., et al. (2017), A representation of the phosphorus cycle for ORCHIDEE (revision 4520), *Geosci.*
 445 *Model Dev.*, 10(10), 3745-3770.
 446 Gong, Y., and J. Wu (2021), Vegetation composition modulates the interaction of climate warming and
 447 elevated nitrogen deposition on nitrous oxide flux in a boreal peatland, *Global Change Biology*, 27(21),
 448 5588-5598.
 449 Harden, J. W., et al. (2012), Field information links permafrost carbon to physical vulnerabilities of
 450 thawing, *Geophysical Research Letters*, 39(15).
 451 Hugelius, G., J. Loisel, S. Chadburn, R. B. Jackson, M. Jones, G. MacDonald, M. Marushchak, D. Olefeldt,
 452 M. Packalen, and M. B. Siewert (2020), Large stocks of peatland carbon and nitrogen are vulnerable to
 453 permafrost thaw, *Proceedings of the National Academy of Sciences*, 117(34), 20438-20446.
 454 Inatomi, M., A. Ito, K. Ishijima, and S. Murayama (2010), Greenhouse gas budget of a cool-temperate
 455 deciduous broad-leaved forest in Japan estimated using a process-based model, *Ecosystems*, 13(3), 472-
 456 483.
 457 Joos, F., R. Spahni, B. D. Stocker, S. Lienert, J. Müller, H. Fischer, J. Schmitt, I. C. Prentice, B. Otto-Bliesner,
 458 and Z. Liu (2020), N₂O changes from the Last Glacial Maximum to the preindustrial – Part 2: terrestrial N₂O
 459 emissions and carbon–nitrogen cycle interactions, *Biogeosciences*, 17(13), 3511-3543.
 460 Kammann, C., C. Müller, L. Grünhage, and H.-J. Jäger (2008), Elevated CO₂ stimulates N₂O emissions in
 461 permanent grassland, *Soil Biology and Biochemistry*, 40(9), 2194-2205.
 462 Liu, S., C. Ji, C. Wang, J. Chen, Y. Jin, Z. Zou, S. Li, S. Niu, and J. Zou (2018), Climatic role of terrestrial
 463 ecosystem under elevated CO₂: a bottom - up greenhouse gases budget, *Ecology letters*, 21(7), 1108-
 464 1118.
 465 Marushchak, M. E., A. Pitkämäki, H. Koponen, C. Biasi, M. Seppälä, and P. J. Martikainen (2011), Hot
 466 spots for nitrous oxide emissions found in different types of permafrost peatlands, *Global Change Biology*,
 467 17(8), 2601-2614.
 468 Marushchak, M. E., J. Kerttula, K. Diáková, A. Faguet, J. Gil, G. Grosse, C. Knoblauch, N. Lashchinskiy, P. J.
 469 Martikainen, and A. Morgenstern (2021), Thawing Yedoma permafrost is a neglected nitrous oxide source,
 470 *Nature communications*, 12(1), 1-10.
 471 Masson-Delmotte, V., P. Zhai, A. Pirani, S. L. Connors, C. Péan, S. Berger, N. Caud, Y. Chen, L. Goldfarb, and
 472 M. I. Gomis (2021), Climate Change 2021: The Physical Science Basis. Contribution of Working Group I to
 473 the Sixth Assessment Report of the Intergovernmental Panel on Climate Change, *IPCC: Geneva,*
 474 *Switzerland*.
 475 Meyerholt, J., K. Sickel, and S. Zaehle (2020), Ensemble projections elucidate effects of uncertainty in
 476 terrestrial nitrogen limitation on future carbon uptake, *Global Change Biology*, 26(7), 3978-3996.
 477 Myers-Smith, I. H., J. T. Kerby, G. K. Phoenix, J. W. Bjerke, H. E. Epstein, J. J. Assmann, C. John, L. Andreu-
 478 Hayles, S. Angers-Blondin, and P. S. Beck (2020), Complexity revealed in the greening of the Arctic, *Nature*
 479 *Climate Change*, 10(2), 106-117.
 480 Nevison, C., A. Andrews, K. Thoning, E. Dlugokencky, C. Sweeney, S. Miller, E. Saikawa, J. Benmergui, M.
 481 Fischer, and M. Mountain (2018), Nitrous oxide emissions estimated with the CarbonTracker - Lagrange
 482 North American regional inversion framework, *Global Biogeochemical Cycles*, 32(3), 463-485.
 483 Nishina, K., A. Ito, N. Hanasaki, and S. Hayashi (2017), Reconstruction of spatially detailed global map of
 484 NH₄⁺ and NO₃⁻ application in synthetic nitrogen fertilizer, *Earth Syst. Sci. Data*, 9(1), 149-162.

Olin, S., M. Lindeskog, T. A. M. Pugh, G. Schurgers, D. Wårlind, M. Mishurov, S. Zaehle, B. D. Stocker, B. Smith, and A. Arneth (2015), Soil carbon management in large-scale Earth system modelling: implications for crop yields and nitrogen leaching, *Earth System Dynamics*, 6(2), 745-768.

Patra, P. K., M. Takigawa, S. Watanabe, N. Chandra, K. Ishijima, and Y. Yamashita (2018), Improved chemical tracer simulation by MIROC4.0-based atmospheric chemistry-transport model (MIROC4-ACTM), *Sola*, 14, 91-96.

Patra, P. K., E. J. Dlugokencky, J. W. Elkins, G. S. Dutton, Y. Tohjima, M. Sasakawa, A. Ito, R. F. Weiss, M. Manizza, and P. B. Krummel (2022), Forward and inverse modelling of atmospheric nitrous oxide using MIROC4-atmospheric chemistry-transport model, *Journal of the Meteorological Society of Japan. Ser. II*.

Pithan, F., and T. Mauritsen (2014), Arctic amplification dominated by temperature feedbacks in contemporary climate models, *Nature Geoscience*, 7(3), 181-184.

Rantanen, M., A. Y. Karpechko, A. Lipponen, K. Nordling, O. Hyvärinen, K. Ruosteenoja, T. Vihma, and A. Laaksonen (2022), The Arctic has warmed nearly four times faster than the globe since 1979, *Communications Earth & Environment*, 3(1), 168.

Ravishankara, A. R., J. S. Daniel, and R. W. Portmann (2009), Nitrous oxide (N₂O): the dominant ozone-depleting substance emitted in the 21st century, *science*, 326(5949), 123-125.

Rees, R. M., J. Augustin, G. Alberti, B. C. Ball, P. Boeckx, A. Cantarel, S. Castaldi, N. Chirinda, B. Chojnicki, and M. Giebel (2013), Nitrous oxide emissions from European agriculture—an analysis of variability and drivers of emissions from field experiments, *Biogeosciences*, 10(4), 2671-2682.

Repo, M. E., S. Susiluoto, S. E. Lind, S. Jokinen, V. Elsakov, C. Biasi, T. Virtanen, and P. J. Martikainen (2009), Large N₂O emissions from cryoturbated peat soil in tundra, *Nature Geoscience*, 2(3), 189-192.

Risk, N., D. Snider, and C. Wagner-Riddle (2013), Mechanisms leading to enhanced soil nitrous oxide fluxes induced by freeze–thaw cycles, *Canadian Journal of Soil Science*, 93(4), 401-414.

Stewart, K. J., M. E. Brummell, R. E. Farrell, and S. D. Siciliano (2012), N₂O flux from plant-soil systems in polar deserts switch between sources and sinks under different light conditions, *Soil Biology and Biochemistry*, 48, 69-77.

Sun, X., X. Han, F. Ping, L. Zhang, K. Zhang, M. Chen, and W. Wu (2018), Effect of rice-straw biochar on nitrous oxide emissions from paddy soils under elevated CO₂ and temperature, *Science of the total environment*, 628, 1009-1016.

Sun, Y., D. S. Goll, J. Chang, P. Ciais, B. Guenet, J. Helfenstein, Y. Huang, R. Lauerwald, F. Maignan, and V. Naipal (2021), Global evaluation of the nutrient-enabled version of the land surface model ORCHIDEE-CNP v1.2 (r5986), *Geoscientific Model Development*, 14(4), 1987-2010.

Thompson, R. L., K. Ishijima, E. Saikawa, M. Corazza, U. Karstens, P. K. Patra, P. Bergamaschi, F. Chevallier, E. Dlugokencky, and R. G. Prinn (2014), TransCom N₂O model inter-comparison—Part 2: Atmospheric inversion estimates of N₂O emissions, *Atmospheric Chemistry and Physics*, 14(12), 6177-6194.

Thompson, R. L., L. Lassaletta, P. K. Patra, C. Wilson, K. C. Wells, A. Gressent, E. N. Koffi, M. P. Chipperfield, W. Winiwarter, and E. A. Davidson (2019), Acceleration of global N₂O emissions seen from two decades of atmospheric inversion, *Nature Climate Change*, 9(12), 993-998.

Tian, H., G. Chen, C. Lu, X. Xu, D. J. Hayes, W. Ren, S. Pan, D. N. Huntzinger, and S. C. Wofsy (2015), North American terrestrial CO₂ uptake largely offset by CH₄ and N₂O emissions: toward a full accounting of the greenhouse gas budget, *Climatic change*, 129(3-4), 413-426.

Tian, H., J. Yang, R. Xu, C. Lu, J. G. Canadell, E. A. Davidson, R. B. Jackson, A. Arneth, J. Chang, and P. Ciais (2019), Global soil nitrous oxide emissions since the preindustrial era estimated by an ensemble of terrestrial biosphere models: Magnitude, attribution, and uncertainty, *Global change biology*, 25(2), 640-659.

Tian, H., R. Xu, J. G. Canadell, R. L. Thompson, W. Winiwarter, P. Suntharalingam, E. A. Davidson, P. Ciais, R. B. Jackson, and G. Janssens-Maenhout (2020), A comprehensive quantification of global nitrous oxide sources and sinks, *Nature*, 586(7828), 248-256.

Tian, H., et al. (2018), The Global N₂O Model Intercomparison Project, *Bulletin of the American Meteorological Society*, 99(6), 1231-1251.

Usyskin-Tonne, A., Y. Hadar, U. Yermiyahu, and D. Minz (2020), Elevated CO₂ has a significant impact on denitrifying bacterial community in wheat roots, *Soil Biology and Biochemistry*, 142, 107697.

Virkkala, A. M., J. Aalto, B. M. Rogers, T. Tagesson, C. C. Treat, S. M. Natali, J. D. Watts, S. Potter, A. Lehtonen, and M. Mauritz (2021), Statistical upscaling of ecosystem CO₂ fluxes across the terrestrial tundra and boreal domain: Regional patterns and uncertainties, *Global Change Biology*, 27(17), 4040-4059.

Voigt, C., R. E. Lamprecht, M. E. Marushchak, S. E. Lind, A. Novakovskiy, M. Aurela, P. J. Martikainen, and C. Biasi (2017a), Warming of subarctic tundra increases emissions of all three important greenhouse gases—carbon dioxide, methane, and nitrous oxide, *Global Change Biology*, 23(8), 3121-3138.

Voigt, C., M. E. Marushchak, R. E. Lamprecht, M. Jackowicz-Korczyński, A. Lindgren, M. Mastepanov, L. Granlund, T. R. Christensen, T. Tahvanainen, and P. J. Martikainen (2017b), Increased nitrous oxide emissions from Arctic peatlands after permafrost thaw, *Proceedings of the National Academy of Sciences*, 114(24), 6238-6243.

Voigt, C., M. E. Marushchak, B. W. Abbott, C. Biasi, B. Elberling, S. D. Siciliano, O. Sonnentag, K. J. Stewart, Y. Yang, and P. J. Martikainen (2020), Nitrous oxide emissions from permafrost-affected soils, *Nature Reviews Earth & Environment*, 1(8), 420-434.

Wagner-Riddle, C., K. A. Congreves, D. Abalos, A. A. Berg, S. E. Brown, J. T. Ambadan, X. Gao, and M. Tenuta (2017), Globally important nitrous oxide emissions from croplands induced by freeze–thaw cycles, *Nature Geoscience*, 10(4), 279-283.

Walker, A. P., M. G. De Kauwe, A. Bastos, S. Belmecheri, K. Georgiou, R. F. Keeling, S. M. McMahon, B. E. Medlyn, D. J. P. Moore, and R. J. Norby (2021), Integrating the evidence for a terrestrial carbon sink caused by increasing atmospheric CO₂, *New Phytologist*, 229(5), 2413-2445.

Wang, X., S. Siciliano, B. Helgason, and A. Bedard-Haughn (2017), Responses of a mountain peatland to increasing temperature: A microcosm study of greenhouse gas emissions and microbial community dynamics, *Soil Biology and Biochemistry*, 110, 22-33.

Watts, J. D., J. S. Kimball, L. A. Jones, R. Schroeder, and K. C. McDonald (2012), Satellite Microwave remote sensing of contrasting surface water inundation changes within the Arctic–Boreal Region, *Remote Sensing of Environment*, 127, 223-236.

Wells, K. C., et al. (2018), Top-down constraints on global N₂O emissions at optimal resolution: application of a new dimension reduction technique, *Atmos. Chem. Phys.*, 18(2), 735-756.

Wilson, C., M. P. Chipperfield, M. Gloor, and F. Chevallier (2014), Development of a variational flux inversion system (INVICAT v1. 0) using the TOMCAT chemical transport model, *Geoscientific Model Development*, 7, 2485-2500.

Yang, G., Y. Peng, M. E. Marushchak, Y. Chen, G. Wang, F. Li, D. Zhang, J. Wang, J. Yu, and L. Liu (2018), Magnitude and pathways of increased nitrous oxide emissions from uplands following permafrost thaw, *Environmental science & technology*, 52(16), 9162-9169.

You, Y., and S. Pan (2020), Urban Vegetation Slows Down the Spread of Coronavirus Disease (COVID - 19) in the United States, *Geophysical Research Letters*, 47(18), e2020GL089286.

Zaehle, S., P. Ciais, A. D. Friend, and V. Prieur (2011), Carbon benefits of anthropogenic reactive nitrogen offset by nitrous oxide emissions, *Nature Geoscience*, 4(9), 601-605.